5th International Conference on Experimental Fluid Mechanics ICEFM 2018 Munich
Munich, Germany, July 2-4, 2018

Temperature Dependence of Heat and Mass Transfer in a Forced Convective Duct Flow with and without Condensation on one Wall

Christian Brückner[1*], Andreas Westhoff[1], Claus Wagner[1,2]

[1] German Aerospace Center (DLR), Institute of Aerodynamics and Flow Technology, Gttingen, Germany
[2] Institute of Thermodynamics and Fluid Mechanics, Technische Universitt Ilmenau, Ilmenau, Germany
[*] christian.brueckner@dlr.de

Abstract

Experiments were conducted to investigate condensation in a convective moist airflow in a vertical duct with one cooled wall. Based on temperature and moisture measurements the heat and mass transfer were determined by means of the thermal balance for fixed temperature differences between inflow, wall and dew point temperatures for $Re = 2000, 4000, 8000$ in a range of wall temperatures $T_{wall} = 1 - 10$ °C. By comparing results obtained in moist airflow with condensation and dry airflow under similar conditions, the impact of the latent heat transfer on the global heat transfer is investigated. While the mass transfer revealed no significant temperature dependence, the condensation heat transfer showed an increase for elevated temperatures. The release of latent heat signficantly changed the heat transfer mechanism due to the release of heat of evaporation and the layer of condensate on the cooled wall.

1 Introduction

Condensation in convective airflows occurs in many technical applications, often with undesirable consequences. For instance, water condensating in the gap between the fuselage and the cabin wall of an aircraft accumulates in the insulation packages, where it decreases the insulation effect, increases the aircraft's weight and enhances corrosion (Zhang et al. (2012)). Moreover, condensation is a potential danger for road traffic, as the mist on the windscreen affects the driver's visibility (Bopp and Peter (2006)).

A fundamental view on the condensation phenomena occuring on a cooled wall is given by the Nusselt theory for filmwise condensation. It is applied to calculate the heat transfer coefficient as a function of film thickness (Nusselt (1916)). The theory is based on the assumption of a static pure steam with an idealised, laminar water film. There are extensions for the theory considering the effects in flowing steam (Nusselt (1916)), steam with non-condensable gas fractions (Hijikata et al. (1984)) and turbulent condensate film flow (Park et al. (1996)).

It is the objective of this study to extend the Nusselt theory for mixed convection of moist air. Observations have shown that the assumption of a continous condensate film has to be dropped in favour of small droplets (Westhoff (2017)). This results in a change of the ratio of convective to conductive heat transport. With the aim to extend Nusselt's model, we investigate the scaling of sensible and latent heat transfer as well as the corresponding mass

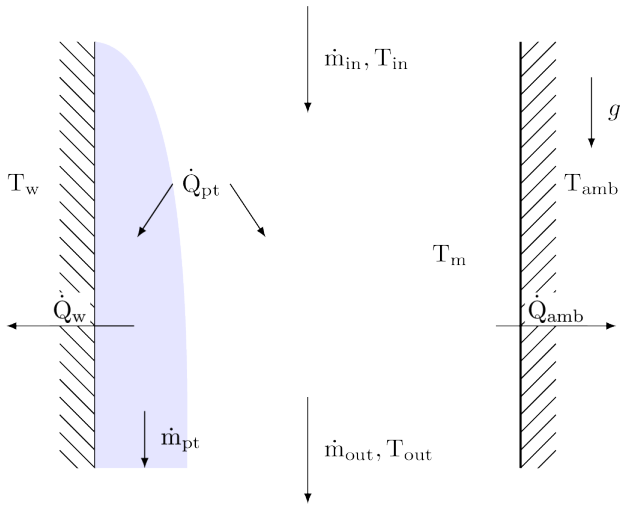

Fig. 1 Sketch of the thermal balance in an adiabatic channel

transfer due to phase transition. For the present study, the scaling of the heat and mass transfer for varying inflow temperatures is evaluated, while the temperature difference between the inlet and the wall temperature and the difference between the dew point and the wall temperature are kept constant.

To calculate the heat transfer, a thermal balance based on an adiabatic channel is introduced as illustrated in Figure 1:

$$\dot{Q}_{in-out} = \dot{Q}_w + \dot{Q}_{pt} + \dot{Q}_{amb} \tag{1}$$

With the heat fluxes being defined as:

$$\dot{Q}_{in-out} = c_p \dot{m}_{air}(T_{in} - T_{out}) \tag{2}$$

$$\dot{Q}_w = \bar{\alpha}_w A_w (T_m - T_w) \tag{3}$$

$$\dot{Q}_{amb} = A_{sw} k_{sw} (T_m - T_{amb}) \tag{4}$$

$$\dot{Q}_{pt} = \dot{m}_{pt} h_v \tag{5}$$

A duct with a high aspect ratio is considered in order to keep the influence of the sidewalls on the flow as small as possible. In Equation 2 $\dot{Q}_{in-out}$ describes the sensible heat transferred from the fluid to the duct with c_p being the heat capacity, $\dot{m}_{air}$ the air mass flow and $(T_{in} - T_{out})$ the difference between inlet and outlet temperatures. Equation 3 describes the heat transfer through the cooled wall $\dot{Q}_w$, where α_w is the combined wall heat transfer coefficient, A_w is the cooled wall surface area and $(T_m - T_w)$ is the difference between mean temperature and cooled wall temperature. $\dot{Q}_{amb}$ in Equation 4 denotes the heat loss through the sidewall with an ambient heat transfer coefficient k_{sw} estimated using the Dittus-Boelter relation (Whitaker (1972)), A_{sw} as the sidewall surface area and $(T_m - T_{amb})$ the difference between the mean and the ambient temperature. $\dot{Q}_{pt}$ is the latent heat, which is equivalent to the amount of condensate (Equation 5) with the condensate mass flow $\dot{m}_{pt}$ and the phase transition enthalpy h_v. To calculate $\dot{Q}_w$ and $\dot{Q}_{amb}$ the mean temperature T_m is required as well as a mean heat transfer coefficient α_w. To work out the mean temperature and heat transfer coefficient, a temperature profile is derived from the thermal balance in Equation 1:

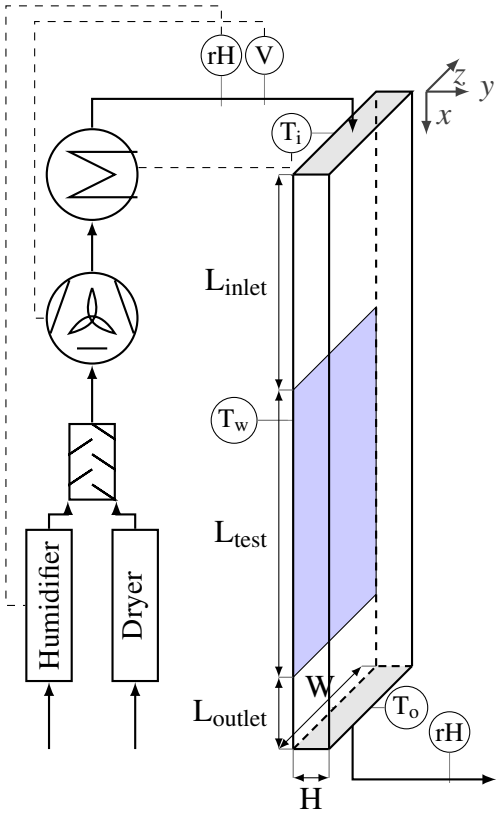

Fig. 2 Block diagram of the vertical duct with conditioning setup

$$\frac{\mathrm{dT}}{\mathrm{dx}} = \frac{(\alpha_w A_w (T(x) - T_w) + \dot{m}_{pt} h_v + A_{sw} k_{sw} (T(x) - T_{amb}))}{c_p \dot{m}_{air}} \tag{6}$$

With an initial guess for the mean temperature the equation is solved with an iteration algorithm. This way, the heat transfer coefficient is calculated to fit with the measured outlet temperature and temperature $T(x)$ averaged over the cross-section can be used to determine the mean temperature T_m for the whole duct.

$$T_m = \frac{1}{L} \int T(x) dx \tag{7}$$

2 Experimental Setup

The measurements are conducted in a vertical duct with an isothermal cooling plate and nearly adiabatic conditions on all other walls (Figure 2). The duct consists of an inlet section to guarantee a well-defined, homogenous inflow and a test and outlet section to ensure an undisturbed flow in the test section. The test section has a length of $L_{test} = 2.05\,\mathrm{m}$, a width of $W = 0.533\,\mathrm{m}$ and a height of $H = 0.05\,\mathrm{m}$ with an aspect ratio of 10.66:1. The temperatures are recorded with resistance thermometers located in the cooling plate, in the ambient air and in the inlet and outlet sections. The dew points are measured with capacitive humidity

Table 1 Parameter overview for constant $\Delta T_{in-w} = 26.5K$, $\Delta T_{dp-w} = 10K$, $Pr = 0.75$, $Ja = 9.33 \times 10^{-3}$ and $Fr = 0.97$

Reynolds number	$\dot{V}_{air}$[1 s^{-1}]	T_{in} [°C]	T_w [°C]	T_{dp} [°C]
2000	9.375			
4000	18.75	27.5 to 35.5	1 to 9	11 to 19
8000	37.5			

sensors and the air mass flow by means of a venturi tube. Based on the measurement data and the thermal balance described in Section 1, the heat fluxes and the mean temperature are determined.

The system is characterised by the Reynolds number $Re = {}^{(U d_{hydr})}/_{\nu}$, Nusselt number $Nu = {}^{(\dot{q} L)}/_{(\lambda_{air} \Delta T)}$, Sherwood number $Sh = {}^{(U_{pt} H)}/_{D}$, Prandtl number $Pr = {}^{(\eta c_p)}/_{\lambda_{air}}$, Froude number $Fr = {}^{U}/_{\sqrt{g' L}}$ and Jakob number $Ja = {}^{(c_p \Delta T_{m-w})}/_{h_v}$. Here, $U = {}^{\dot{V}_{air}}/_{A_{\mathrm{HB}}}$ denotes the average velocity as the ratio of airflow $\dot{V}_{air}$ to duct cross section A_{HB}, d_{hydr} the hydraulic diameter of the duct, ν the kinematic viscosity, $\dot{q}$ the heat flux, $U_{pt} = {}^{\dot{V}_{pt}}/_{A_{pt}}$ the condensation speed as ratio of condensate volume $\dot{V}_{pt}$ to condensation area A_{pt}, D the diffusion coefficient for moist air, λ_{air} the thermal conductivity, $\Delta T = T_{in} - T_{out}$ the characteristic temperature difference between inlet and outlet temperature, η the dynamic viscosity, c_p the heat capacity, g' the bouyancy-corrected gravity and h_v the heat of evaporation.

To describe the lateral heat transfer in air, a second Nusselt number is defined as the ratio of condensate heat transfer to conductive heat transfer $Nu_{pt} = {}^{(\dot{q}_{pt} H)}/_{(\lambda_{air} \Delta T_{(m-w)})}$ with the difference between the mean air temperature and the cooled wall temperature.

To identify the scaling of heat and mass transfer, the Nusselt number and Sherwood number are recorded as a function of different absolute temperatures at the inlet T_{in}, the cooled wall T_w and the dew point T_{dp}. A parameter study is performed for cooled wall temperatures in the range of 1 °C to 10 °C at three Reynolds numbers $Re = 2000/4000/8000$, $\Delta T_{in-w} = 26.5K$, $\Delta T_{dp-w} = 10K$, $Pr = 0.75$, $Ja = 9.33 \times 10^{-3}$ and $Fr = 0.97$ (see Table 1). In addition, measurements with dry air and thus without phase transition are performed for $Re = 4000$ in order to identify the impact of the latent heat on the global heat transfer. All experiments are performed under steady-state conditions for at least 3 h to achieve a thermal equilibrium

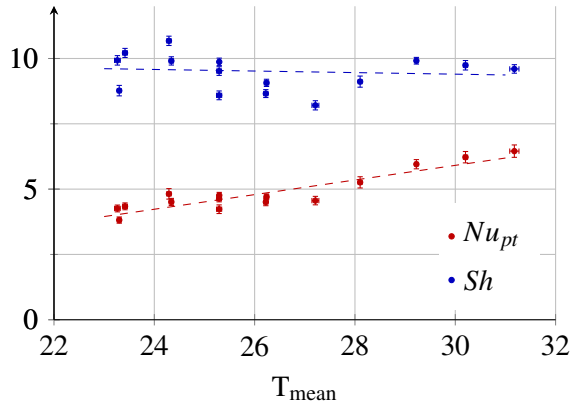

Fig. 3 Temperature dependence of Sherwood (blue) and condensation Nusselt number (red) at $Re = 4000$

3 Temperature Dependence of Nusselt and Sherwood Numbers

Figure 3 shows the Sherwood numbers (blue) and condensation Nusselt numbers (red) plotted as a function of the mean temperature T_m for $Re = 4000$. The linear regression slope of $-0.03\,\mathrm{K}^{-1}$ displays that the Sherwood number is almost temperature independent. This independency indicates that the increasing vapour mass transfer due to phase transition on the cooled surface and the corresponding mass transfer due to diffusion from the bulk into the boundary above the cooled surface are of the same magnitude.

Analogously, the relative condensate mass ${}^{\dot{m}_{pt}}/_{\dot{m}_{water}}$ with $\dot{m}_{water}$ being the total water content of the moist air, is constant. This reveales no dependency on the temperature for the mass transfer mechanisms. On this basis we expect that for this Reynolds number the Sherwood number is predominantly affected by the temperature differences, as it is the driving force for the condensation mass transfer. In contrast to the Sherwood number, the condensation Nusselt number, representing the lateral heat transfer through condensation, increases with increasing temperatures with a slope of $0.28\,\mathrm{K}^{-1}$. This is a direct result of

the rise in heat of evaporation due to the higher condensate mass m_{pt} at elevated mean temperatures T_{mean}. With higher water content, the latent heat transfer becomes more important than the change in sensible heat transfer, as the increase in heat of evaporation exceeds the increase of the heat conductivity of air.

At a lower Reynolds number of $Re = 2000$, a decrease of the Sherwood number is observed for higher temperatures with a slope of $-0.123\,\mathrm{K}^{-1}$ (Figure 4). This indicates that the influence of diffusive mass transfer at this Reynolds number is larger at higher temperatures. A possible explanation for this observation is a laminar flow. The condensation Nusselt number is slightly higher than for the case $Re = 4000$, which is consistent with an expected lower heat conduction in the assumed laminar flow. The comparison to the higher Reynolds number further reveals a slightly higher slope of $0.233\,\mathrm{K}^{-1}$, which can be attributed to the increased influence of the diffusive mass transfer. In principle, lower fluid temperatures are observed for lower velocities due to the increased heat transfer, which is the result of a longer dwell time. At $Re = 8000$, where the flow is assumed to be fully turbulent, the higher Sherwood number reflects that the convective mass transfer dominates over the diffusive mass transfer (see Figure 5). Additionally, the Sherwood number increases with increasing mean temperatures with a regression slope of $0.09\,\mathrm{K}^{-1}$. The latent heat transfer increases for higher velocity and the dependency on the mean temperature becomes more significant, indicated by the regression slope of $0.53\,\mathrm{K}^{-1}$. This effect can be explained by the increased level of turbulence, which enhances mixing. As a consequence, the mass transport of vapour into the boundary layer above the cooled surface is enhanced. The results is the increased mass transfer due to phase transition. Contrary to the lower Re case, the mean temperatures are higher due to shorter dwell times.

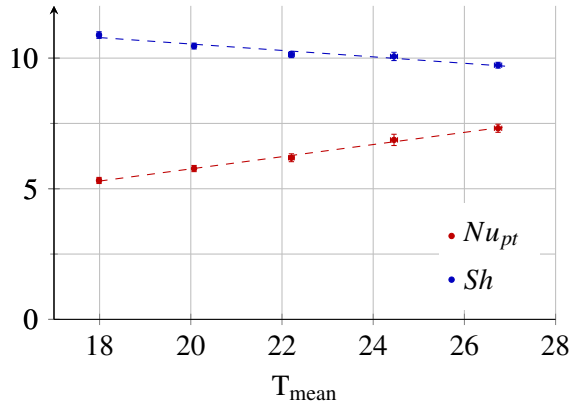

Fig. 4 Temperature dependence of Sherwood (blue) and condensation Nusselt number (red) at $Re = 2000$

4 Impact of Latent Heat Release on the Heat Transfer

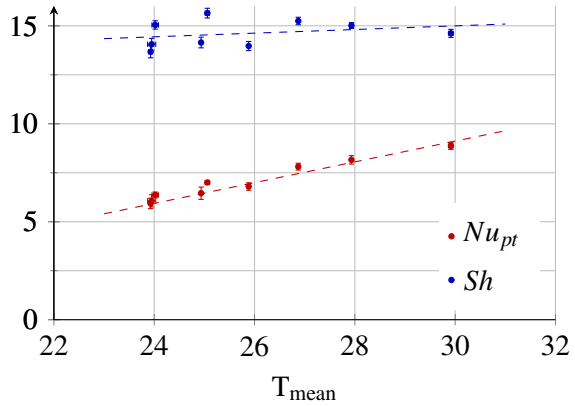

Fig. 5 Temperature dependence of Sherwood (blue) and condensation Nusselt number (red) at $Re = 8000$

To evaluate the impact of the latent heat, the results for moist air and dry air at $Re = 4000$ are compared. Figure 6 shows the dimensionless temperature profiles $T'_x = {}^{(T_x - T_{out})}/_{(T_{in} - T_{out})}$ over the dimensionless duct length $L' = {}^{L_x}/_{(Re_{hydr} * Pr * d_{hydr})}$ averaged for the case of dry air (red) and averaged for the case of moist air (blue) derived from the thermal balance (see Section 1). The mean temperature observed over the duct length is lower in case of the dry airflow, which indicates the impact of latent heat release on the global heat transfer and the additional heat resistance resulting from the condensate layer. Both effects lead to a nearly 3 % higher outlet temperature in case of airflow with condensation.

The global heat transfer is calculated by adding up latent and sensible heat transfer. In Figure 7 it is plotted for the moist air case (blue squares) and dry air case (red squares). For the moist air case the sensible heat is displayed separatly (blue triangles) to highlight the particular shares of latent and sensible heat. It is evident that even though the outlet temperature is higher in the moist air case, the heat transfer is increased. The sensible heat transfer is reduced in the case of moist air, which further

indicates the inhibition of convective heat transfer as a result of the added layer of thermal resistance. In addition, the limited heat transfer through the cooled wall also leads to a higher outlet temperature. On a microscale this means that when the specific heat of evaporation for one droplet is released, the limited heat transfer causes a fraction of the latent heat to be returned to the fluid. This local heat transfer reduces the overall sensible heat transfer detected by the thermal balance compared to the case with dry air.

Figure 7 also reveals that while the sensible heat transfer is independent of the temperature, condensation leads to a temperature dependence for the global heat transfer. This confirms the findings that the latent heat transfer predominantly increases the global heat transfer with rising temperatures, as described in Section 3. The global heat transfer is significantly limited by the heat transfer through the condensation surface.

Assuming that a fraction of the latent heat is released back into the fluid, we can modify the thermal balance (Equation 1). The latent heat is divided into the part that is transported through the cooled wall $\dot{Q}^w_{pt}$ and the part that is returned to the fluid $-\dot{Q}^f_{pt}$, which add to $\dot{Q}_{pt} = \dot{Q}^w_{pt} + \dot{Q}^f_{pt}$:

$$\dot{Q}_{in-out} = \underbrace{(\dot{Q}^s_w + \dot{Q}^w_{pt})}_{\dot{Q}_w} - \dot{Q}^f_{pt} + \dot{Q}_{amb} \qquad (8)$$

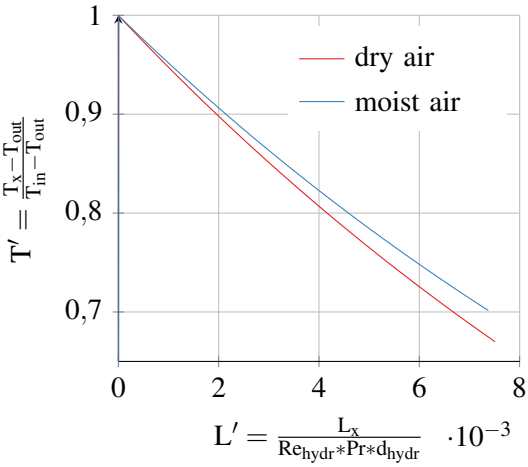

Fig. 6 Comparison of average temperature profiles at Re = 4000 with and without condensation

$\dot{Q}^s_w$ is the sensible heat transported through the wall. By comparing the fractions of latent heat determined by Equation 8, it is found that an average of 39.1 % of the latent heat is released back into the air for $Re = 4000$. While there are no dry air measurements for $Re = 8000$, based on the thermal balance for the moist air case it is found that 33 % of latent heat are released back into the air. This ratio does not depend on the temperature for both cases.

This finding illustrates the link between heat transfer and flow velocity. The near-wall flow structures are influenced by the changed surface structure due to droplet deposition on the wall. Since these structures depend heavily on the flow regime, a further investigation of the velocity dependence of the heat transfer is necessary

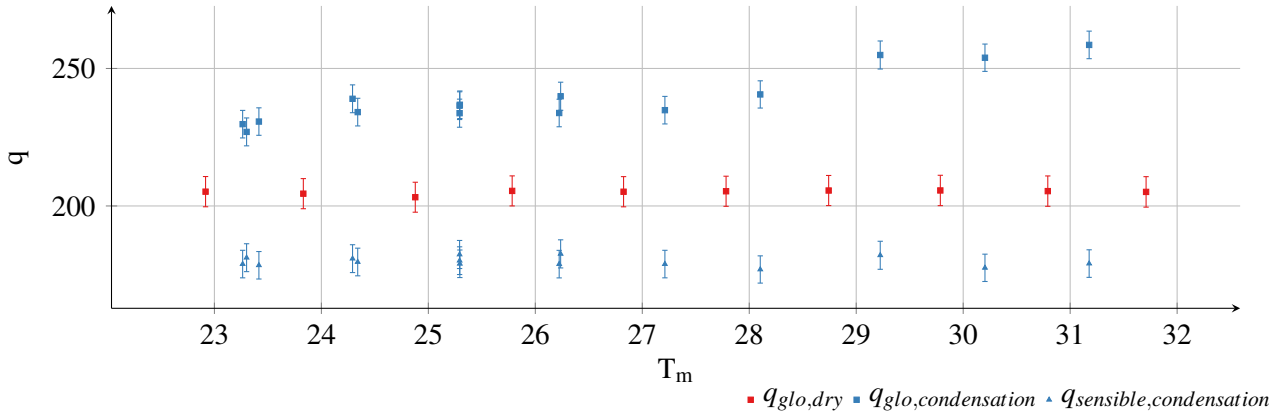

Fig. 7 Comparison of global heat transfer to the channel with and without condensation

5 Conclusion

In this study the latent and sensible heat transfer as well as the corresponding mass transfer in a convective moist airflow characterised by the dimensionless condensation Nusselt number and Sherwood number were determined as a function of the mean temperature at steady-state conditions. With increasing temperatures the Sherwood number decreases for $Re = 2000$, remains almost constant for $Re = 4000$ and increases slightly for $Re = 8000$. This behaviour is attributed to the larger influence of diffusive mass transfer in laminar flow. For turbulent flow at $Re = 8000$ the convective mass transfer is dominant with a 50 % higher Sherwood number. The condensation Nusselt number increases with higher temperatures in all three cases with elevating slopes for higher Reynolds numbers. This reflects the increasing water content carried by the moist air with increasing temperatures and is further enhanced by increasing levels of turbulence.

The comparison between dry air and moist air under similar conditions revealed that a significant part of the latent heat is released back into the airflow. The reasons for this phenomenon are a limited heat transfer through the cooled wall, an additional heat transfer resistance caused by the added layer of condensate and interference with the convective flow structures near the wall through the droplet deposition on the cooled wall.

References

Bopp R and Peter A (2006) Windshield fogging in road tunnels - final results. in *3rd International Conference Tunnel Safety and Ventialtion*. pages 232–239. Graz

Hijikata K, Chen S, and Tien C (1984) Non-condensable gas effect on condensation in a two-phase closed thermosyphon. *International Journal of Heat and Mass Transfer* 27:1319–1325

Nusselt W (1916) Die Oberflächenkondensation des Wasserdampfes. *Zeitschrift des Vereins Deutscher Ingenieure* 60:541–546

Park SK, Kim MH, and Yoo KJ (1996) Condensation of pure steam and steam-air mixture with surface waves of condensate film on a vertical wall. *International Journal of Multiphase Flow* 22:893–908

Westhoff A (2017) Experimentelle Untersuchung des Einflusses der Oberflächenbeschaffenheit von Scheiben auf die Kondensatbildung. Technical Report 303

Whitaker S (1972) Forced Convection Heat Transfer Correlations for Flow In Pipes, Past Flat Plates, Single. *AIChE Journal* 18:361–371

Zhang TT, Tian L, Lin CH, and Wang S (2012) Insulation of commercial aircraft with an air stream barrier along fuselage. *Building and Environment* 57:97–109